

Invited Review

Comparative anatomy of respiratory bronchioles and lobular structures in mammals

Yumi Umeda^{1*a}, Takeshi Izawa^{2a}, Kei Kazama³, Sachiko Arai³, Junichi Kamiie⁴, Shinichiro Nakamura⁵, Kazuki Hano⁶, Masaki Takasu^{6,7}, Akihiro Hirata^{7,8}, Susanne Rittinghausen⁹, and Shotaro Yamano^{1*}

¹ National Institute of Occupational Safety and Health, Japan, Organization of Occupational Health and Safety, 2-26-1 Muraoka-higashi, Fujisawa, Kanagawa 251-0015, Japan

² Laboratory of Veterinary Pathology, Osaka Metropolitan University Graduate School of Veterinary Science, 1-58 Rinku-Orai-Kita, Izumisano, Osaka 598-8531, Japan

³ Department of Veterinary Medicine, Azabu University, School of Veterinary Medicine, 17-71 Fuchinobe 1-chome, Chuo-ku, Sagamihara 252-5201, Japan

⁴ Laboratory of Veterinary Pathology, School of Veterinary Medicine, Azabu University, 1-17-71 Fuchinobe, Chuo-ku, Sagamihara, Kanagawa 252-5201, Japan

⁵ Laboratory of Laboratory Animal Science, School of Veterinary Medicine, Azabu University, 1-17-71 Fuchinobe, Chuo-ku, Sagamihara, Kanagawa 252-5201, Japan

⁶ Gifu University Institute for Advanced Study, Gifu University, 1-1 Yanagido, Gifu 501-1193, Japan

⁷ Center for One Medicine Innovative Translational Research (COMIT), Gifu University, 1-1 Yanagido, Gifu, 501-1193, Gifu, 501-1193, Japan

⁸ Laboratory of Veterinary Pathology, Joint Department of Veterinary Medicine, Faculty of Applied Biological Sciences, Gifu University, 1-1 Yanagido, Gifu, 501-1193, Japan

⁹ Fraunhofer Institute for Toxicology and Experimental Medicine (ITEM), Nikolai-Fuchs-Strasse 1, 30625, Hannover, Germany

Abstract: Rodents are widely used to study the toxicity of chemicals; however, differences between species indicate that the results from rodents are not always directly transferable to humans. The health of workers exposed to various chemicals and particulates at high doses or for long periods is at risk. Respiratory bronchioles and lobular structures, which are demarcated by interlobular septa, are key sites for occupational lung diseases such as pneumoconiosis; however, these structures vary among animal species. Understanding these differences is crucial for studying the pathology of human occupational lung diseases. However, there is a lack of reviews focusing on these structures in different species. This review explores the lung anatomy of various mammals and its functional importance in disease to connect animal studies with human occupational lung diseases. Our results indicate that artiodactyls, especially small pig breeds and goats, are ideal for research because their respiratory bronchioles and lobular structures are similar to those of humans. This review aims to enhance the use of experimental animal data and improve our understanding of human occupational lung diseases, thereby facilitating early disease detection, treatment, and prevention. (DOI: 10.1293/tox.2024-0071; J Toxicol Pathol 2025; 38: 113–129)

Key words: comparative anatomy, respiratory bronchiole, lobular structure, interlobular septum, lung

Introduction

Rodents, such as rats and mice, are the most commonly used animals for studying chemical toxicity. However, species differences must be considered when applying findings from rodents to humans. Several studies have compared animal and human lungs in terms of gas exchange and ventilation^{1, 2}, tissue responses to particulate toxicity³, particulate deposition and clearance⁴, and lung high-resolution computed tomography images⁵. Research using genetically modified mice for lung stem cell studies^{6–9} has highlighted the anatomical differences between mouse and human lungs⁶. Animals with different lung anatomies may not be appropriate models for human lung diseases. An accurate understanding of lung structure and cellular composition is

Received: 20 August 2024, Accepted: 19 December 2024

Published online in J-STAGE: 2 January 2025

^aYumi Umeda and Takeshi Izawa have contributed equally to this work.

*Corresponding authors:

Y Umeda (e-mail: umeda-yumi@h.jniiosh.johas.go.jp);

S Yamano (e-mail: shotaro-yamano@pulmpath.com)

©2025 The Japanese Society of Toxicologic Pathology

This is an open-access article distributed under the terms of the Creative Commons Attribution Non-Commercial No Derivatives



(by-nc-nd) License. (CC-BY-NC-ND 4.0: <https://creativecommons.org/licenses/by-nc-nd/4.0/>).

essential in order to establish suitable experimental animal models for evaluating chemical/particulate toxicity and understanding lung disease pathology.

Workplaces are key settings where exposure to chemicals or particulates can occur. Workers exposed to high concentrations or for prolonged periods of time to various chemicals are at risk of developing lung diseases, including pneumoconiosis, which is an occupational lung disease caused by the inhalation of dust and fibers. Early symptoms may be absent and not everyone exposed will develop lung lesions, leading to a lack of recognition of the developing disease and resulting in diagnosis only at advanced stages of the disease¹⁰. Therefore, appropriate experimental animals are needed for the accurate understanding, early detection, treatment, and prevention of pneumoconiosis and other lung diseases resulting from the inhalation of toxic chemicals/particulates. Respiratory bronchioles are notably affected by particle deposition, particularly in coal miners^{11, 12}. Asbestosis, silicosis, and mixed-dust fibrosis, the most common forms of pneumoconiosis, are characterized by significant fibrosis of the respiratory bronchioles and alveolar ducts^{12–16}. The lymphatic system of the lungs removes inflammatory cells and damaged tissue caused by particulate matter and microorganisms¹⁷, with the subpleural and interlobular lymphatics being the main routes¹⁸. Computed tomography (CT) imaging of pneumoconiosis often shows small nodules in the centrilobular regions and thickened interlobular septa¹⁹, indicating incomplete removal of the deposited material and the importance of lung anatomy.

Changes in the lungs of Japanese workers exposed to cross-linked water-soluble acrylic acid polymers (CWAAP) suggest pneumoconiosis. Although inorganic dust is known to cause pneumoconiosis, there is no established evidence supporting the effects of organic dust on pneumoconiosis. Therefore, further research on CWAAP-induced disease is required. Workers inhaling CWAAP showed fibrosis in the respiratory bronchioles and pleural and interlobular septal fibrosis²⁰. In rats, changes are limited to the alveolar regions, with interstitial fibrosis of the alveolar septa^{21, 22}. Although fibrosis was noted, the development of fibrosis and the causative factors may differ between rats and humans, as fibrosis develops in different areas of the lungs in rats and humans. Therefore, animals with respiratory bronchioles and interlobular septa similar to those in humans are required to study this pathology.

In this review, the definitions of respiratory bronchioles and lobular structures are based on the studies by Peake and Pinkerton²³, Miller²⁴, and Reid²⁵. Briefly, respiratory bronchioles are defined as the transition zone between the conducting airways and respiratory air spaces²³. They have structures similar to those of the non-respiratory bronchioles, except for the presence of openings for alveoli in their walls and shorter epithelial cells. Secondary lobules, as proposed by Miller²⁴ and Reid²⁵, are defined as the smallest units of the lung structure and are bordered by connective tissue septa (interlobular septa). In addition, the interlobular septa extend to the pleura, and under macroscopic observa-

tion, they appear as polygonal patterns on the lung surface.

Comparative anatomical studies of respiratory bronchioles and pulmonary lobule structures are crucial for understanding human occupational respiratory diseases. This will also benefit researchers studying human respiratory diseases. However, comprehensive reviews that focus on these structures in different animal species are limited²³. This review aims to provide an overview of the morphology and function of human respiratory bronchioles and pulmonary lobule structures and to detail these structures in different animals to identify the best animal models for studying occupational respiratory diseases.

Material Used for the Overview of the Lung Histology

All animal species presented in this review are listed in Tables 1 and 2. Gross and histopathological images using H&E-stained slides were observed for the animal species listed in Table 1.

Lung tissues of rats and mice were provided by the Japan Bioassay Research Center; Microminipig lung tissues were provided by Gifu University; domestic pig, goat, cynomolgus monkey, and cow lung tissues were provided by Azabu University; beagle dog and cynomolgus monkey tissues were provided by Shin Nippon Biomedical Laboratories, Ltd.; and naked mole-rat lung tissues were provided by Kumamoto University. Whole-slide images of the gray squirrel, chinchilla, capybara, squirrel monkey, goat, reindeer, alpaca, donkey, pantropical spotted dolphin, black rhinoceros, Bengal tiger, Japanese raccoon dog, Chinese wolf, and koala were provided by Osaka Metropolitan University.

Information regarding the presence or absence of respiratory bronchioles and interlobular septa was obtained from published articles (Table 2)^{23, 26–31}.

Morphology and Function of Human Bronchioles and Lung Lobular Structure

The human trachea forms a complex system of branching airways known as the bronchial tree, which undergo approximately 23 divisions³². As these airways branch, their number increases and their diameters decrease. In the peripheral airways, including the respiratory bronchioles, the cross-sectional area and total volume increase dramatically, slowing the airflow until it nearly stops at the periphery³³. Most airways are lined with pseudostratified ciliated epithelial cells, which decrease in height towards the periphery. The airway mucosa includes goblet, serous, and acinar cells in the submucosal glands³⁴. The coordinated activity of cilia and goblet cell secretions forms the mucociliary escalator, which is essential for removing inhaled particles from the lungs. The alveolar epithelium consists mainly of type I alveolar epithelial cells for gas exchange and type II alveolar epithelial cells for surfactant production. Alveolar macrophages process and remove inhaled particles, initiate immune responses, and protect the alveoli³⁵.

Table 1. Presence or Absence of Respiratory Bronchioles and Interlobular Septa in Mammals

Order	Species	Macroscopic image	Microscopic image	
		Polygonal pattern	Interlobular septa	Respiratory bronchioles
Rodents	rat (<i>Rattus norvegicus</i>)	X	X	X
	mouse (<i>Mus musculus</i>)	X	X	X
	naked mole-rat (<i>Heterocephalus glaber</i>)	X	X	X
	gray squirrel (<i>Sciurus carolinensis</i>)	NA	X	X
	chinchilla (<i>Chinchilla lanigera</i>)	X	X	X
	capybara (<i>Hydrochoerus hydrochaeris</i>)	X	X	○
Primates	cynomolgus monkey (<i>Macaca fascicularis</i>)	X	X	◎
	common marmoset (<i>Callithrix jacchus</i>)	X	X	◎
	squirrel monkey (<i>Saimiri sciureus</i>)	— a	X	◎
Cetartiodactyla	microminipig (<i>Sus scrofa domesticus</i>)	○	◎	○
	domestic pig (<i>Sus scrofa domesticus</i>)	○	◎	○
	goat (<i>Capra Linnaeus</i>)	○	○	◎
	cow (<i>Bos taurus</i>)	○	◎	◎
	reindeer (<i>Rangifer tarandus</i>)	○	◎	○
	alpaca (<i>Vicugna pacos</i>)	○	○	○
	pantropical spotted dolphin (<i>Stenella attenuata</i>)	X	X	X
Perissodactyla	donkey (<i>Equus asinus</i>)	○	○	— b
	black rhinoceros (<i>Diceros bicornis</i>)	○	○	— b
Carnivora	dog (<i>Canis familiaris</i>)	X	X	◎
	Bengal tiger (<i>Panthera tigris tigris</i>)*	X	X	◎
	Japanese raccoon dog (<i>Nyctereutes viverrinus viverrinus</i>)	X	X	◎
	Chinese wolf (<i>Canis lupus chanco</i>)	X	X	◎
Marsupialia	koala (<i>Phascolarctos cinereus</i>)**	X	X	— b

◎: Remarkable; ○: Present; X: Absent; —: Unable to determine; NA: Data not available; a: Congestion and hemorrhage; b: Not determine due to unclear bronchiole structure in the prepared specimen. *: Published as a case report; Kuramochi M, Izawa T, Hori M, *et al.* Chordoma of the thoracic vertebrae in a Bengal tiger (*Panthera tigris tigris*). J Vet Med Sci. 2015 Jul;77(7):893–5. doi: 10.1292/jvms.14-0658. **: Published as a case report; Kuwamura M, Murai F, Nishioka S, *et al.* Late onset cerebellar cortical degeneration in a koala. Aust Vet J. 2009 Aug;87(8):342–4. doi: 10.1111/j.1751-0813.2009.00463.x.

Table 2. Presence or Absence of Respiratory Bronchioles and Interlobular Septa in Mammals from the Literature

Order	Species	Literature information		References
		Lobular septa	Respiratory bronchioles	
Primates	human (<i>Homo sapiens</i>)	Extensive	1–3 generations	23
	rhesus monkey (<i>Macaca mulatta</i>)	Few	Several	23, 26
Rodents	gerbil (<i>Meriones unguiculatus</i>)	Few or none	Absent or poorly developed	23
	hamster (<i>Mesocricetus auratus</i>)	Few or none	Absent or poorly developed	23
	guinea pig (<i>Cavia porcellus</i>)	Few or none	Absent or poorly developed	23
	rabbit (<i>Oryctolagus cuniculus</i>)	Few or none	Absent or poorly developed	23
Cetartiodactyla	camel (<i>Camelus dromedarius</i>)	Exist	Present	27–29
	sheep (<i>Ovis aries</i>)	Extensive	Absent or poorly developed	23
Perissodactyla	horse (<i>Equus caballus</i>)	Extensive	Absent	30
Carnivora	cat (<i>Felis catus</i>)	Few or none	Several	23
	ferret (<i>Mustela putorius furo</i>)	Few	Several	23, 31

Respiratory bronchioles, located between the terminal bronchioles and alveolar ducts, give rise to alveoli. This region is prone to specific lesions due to 1) areas of poor ventilation where fine particles accumulate, potentially affecting nearby respiratory bronchioles; 2) being a transitional zone where air moves between narrow and wide spaces, causing complex airflow and stasis; and 3) the lack of cilia in respiratory bronchiolar epithelial cells, making clearance less effective. These factors make respiratory bronchioles sites of potential vulnerability in the lung; for example, respiratory bronchioles are a common site for diffuse lung diseases, such as pneumoconiosis. Therefore, studying occupational respiratory diseases in animals without respiratory bronchioles may lead to an underestimation of the impact of inhaled chemicals and particulates in humans.

The interlobular septa, which are connective tissue sheaths extending from the pleura to the lung parenchyma, contain lymphatic vessels and veins¹². Pulmonary lymphatic vessels protect the lungs from airborne particles and microorganisms, allow fluid influx, and remove foreign substanc-

es and damaged tissues, thereby keeping the lungs clean. Impairment of this function may lead to the development of lesions. Thickening of the interlobular septa is a common feature in CT images of patients with pneumoconiosis¹⁹. The presence of lobular structures may have a significant impact on the morphology of lung lesions. Therefore, studying occupational respiratory diseases in animals with lobular structures is crucial for understanding the histopathology of human lung diseases.

This review examined the presence or absence of respiratory bronchioles and lobular structures in the lungs of various experimental and domestic animals. Based on the findings of our research (Table 1) and the existing literature (Table 2), we discuss the optimal animal species for studying occupational respiratory diseases in humans.

Rodents

Rats (*Rattus norvegicus*) and mice (*Mus musculus*) are commonly used laboratory animals. Their lungs do not

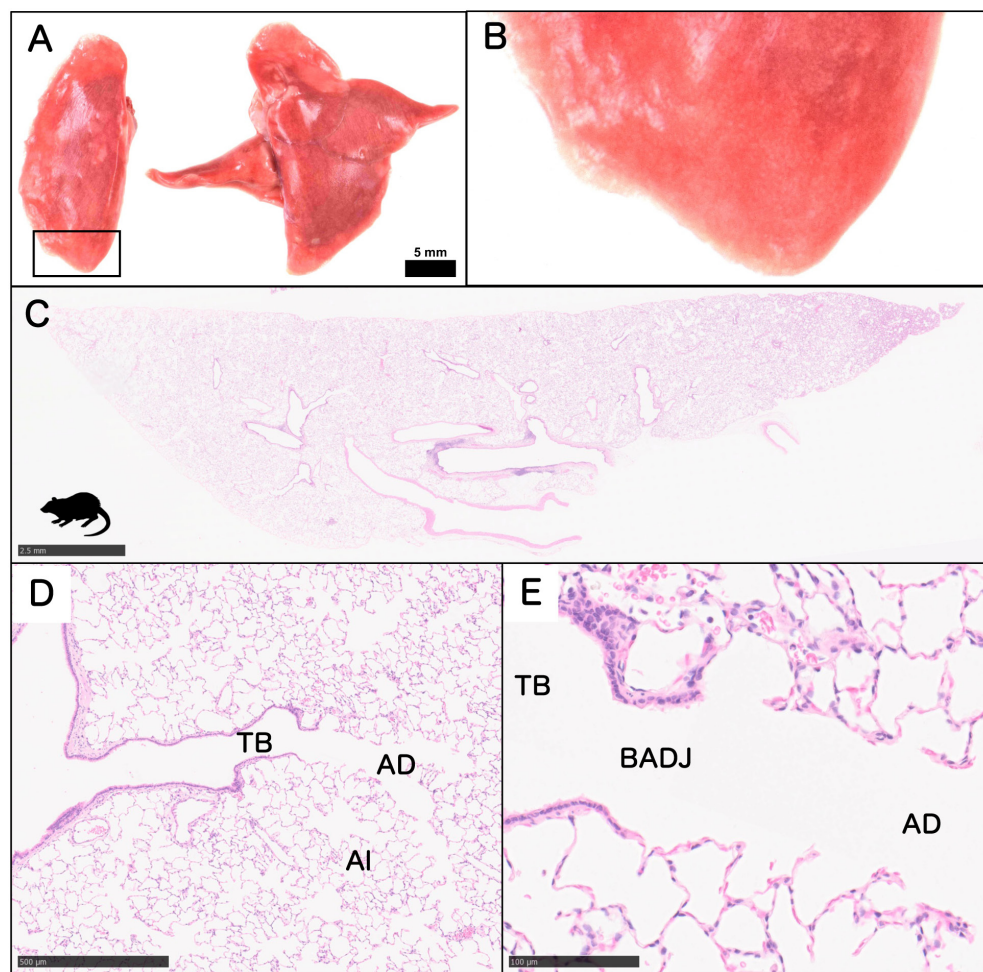


Fig. 1. Macroscopic and microscopic images of the rat lung. A: Macroscopic image of a rat lung. B: Magnified view of the boxed area in panel A. No polygonal patterns can be observed. C: Overall histopathological view of the left lung. D: High-magnification image of Fig. 1C showing the boundary between the bronchioles and alveoli. E: High-magnification image of Fig. 1D. AD: alveolar duct; AI: alveoli; BADJ: bronchiole-alveolar duct junction; TB: terminal bronchiole.

contain respiratory bronchioles or lobular structures. Although human lungs exhibit a polygonal pattern on the surface due to lobular structures, this pattern is absent in rats (Fig. 1A, 1B) and mice (Fig. 2A, 2B). Microscopic examination fails to reveal connective tissue separating the lobules in these rodents (Fig. 1C, Fig. 2C). Therefore, the lobular structures observed in humans are absent in rats and mice. Figures 1 and 2 show the lack of respiratory bronchioles in rats (Fig. 1D, 1E) and mice (Fig. 2D, 2E). Furthermore, their visceral pleura and interstitial connective tissue are relatively thin compared to domestic animals and nonhuman primates³⁶. Notably, our inhalation studies with rats and mice using nanomaterials such as indium tin oxide particles³⁷, multi-walled carbon nanotubes^{38–40}, and titanium dioxide nanoparticles^{41, 42} revealed no interlobular septa lesions or identifiable lobular structure lesions.

To identify rodents with lung structures that are more similar to those of humans, we studied rodents other than rats and mice. In the naked mole-rat (*Heterocephalus glaber*), the longest-living rodent with a lifespan of approxi-

mately 30 years, the lung surface does not exhibit a polygonal pattern during gross examination (Fig. 3A). Histological examination also shows no interlobular septa or respiratory bronchioles (Fig. 3B, 3C, and 3D). Similarly, the gray squirrel (*Sciurus carolinensis*) and chinchilla (*Chinchilla lanigera*) (Table 1), gerbil (*Meriones unguiculatus*), hamster (*Mesocricetus auratus*), guinea pig (*Cavia porcellus*), and rabbit (*Oryctolagus cuniculus*)²³ (Table 2) also lack both interlobular septa and respiratory bronchioles. The capybara (*Hydrochoerus hydrochaeris*), the largest rodent with a body weight of 47 kg, also does not exhibit a polygonal pattern or interlobular septa on the lung surface (Fig. 4A, 4B). However, respiratory bronchioles are observed in the capybara, making it the only rodent in this study with such a feature (Table 1, Fig. 4C).

Beagle Dogs and Other Carnivores

In the beagle dog (*Canis lupus familiaris*), which is often used in research, the polygonal pattern observed in

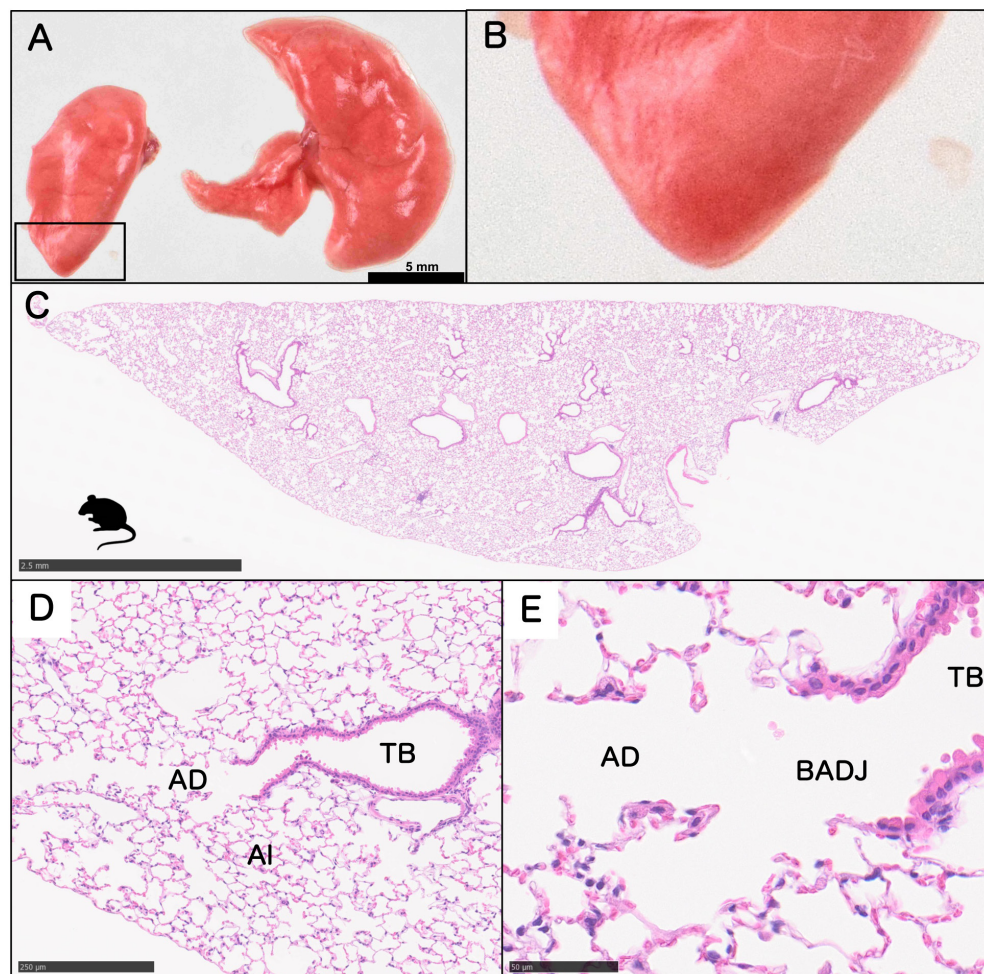


Fig. 2. Macroscopic and microscopic images of the mouse lung. A: Macroscopic image of a mouse lung. B: Magnified view of the boxed area in panel A. No polygonal patterns can be observed. C: Overall histopathological view of the left lung. D: High-magnification image of Fig. 2C showing the boundary between the bronchioles and alveoli. E: High-magnification image of Fig. 2D. AD: alveolar duct; Al: alveoli; BADJ: bronchiole-alveolar duct junction; TB: terminal bronchiole.

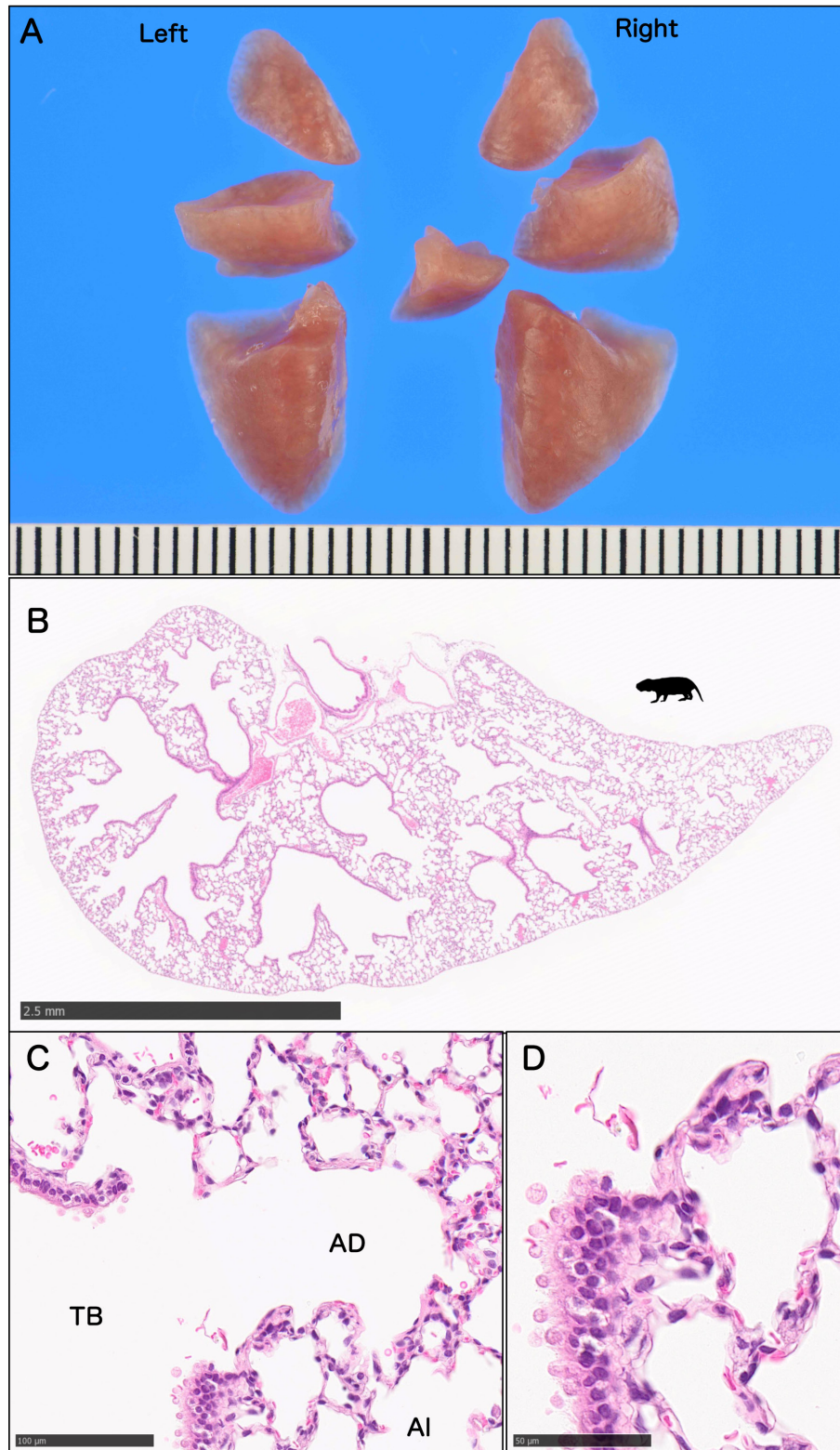


Fig. 3. Macroscopic and microscopic images of the naked mole-rat lung. A: Macroscopic lung structure (left, 3 lobes; right, 4 lobes). B: Microscopic view of the lung. C: High-magnification image of Fig. 3B showing the boundary between the bronchioles and alveoli. D: High-magnification image of Fig. 3C. AD: Alveolar duct; AI: alveoli; TB: terminal bronchiole.

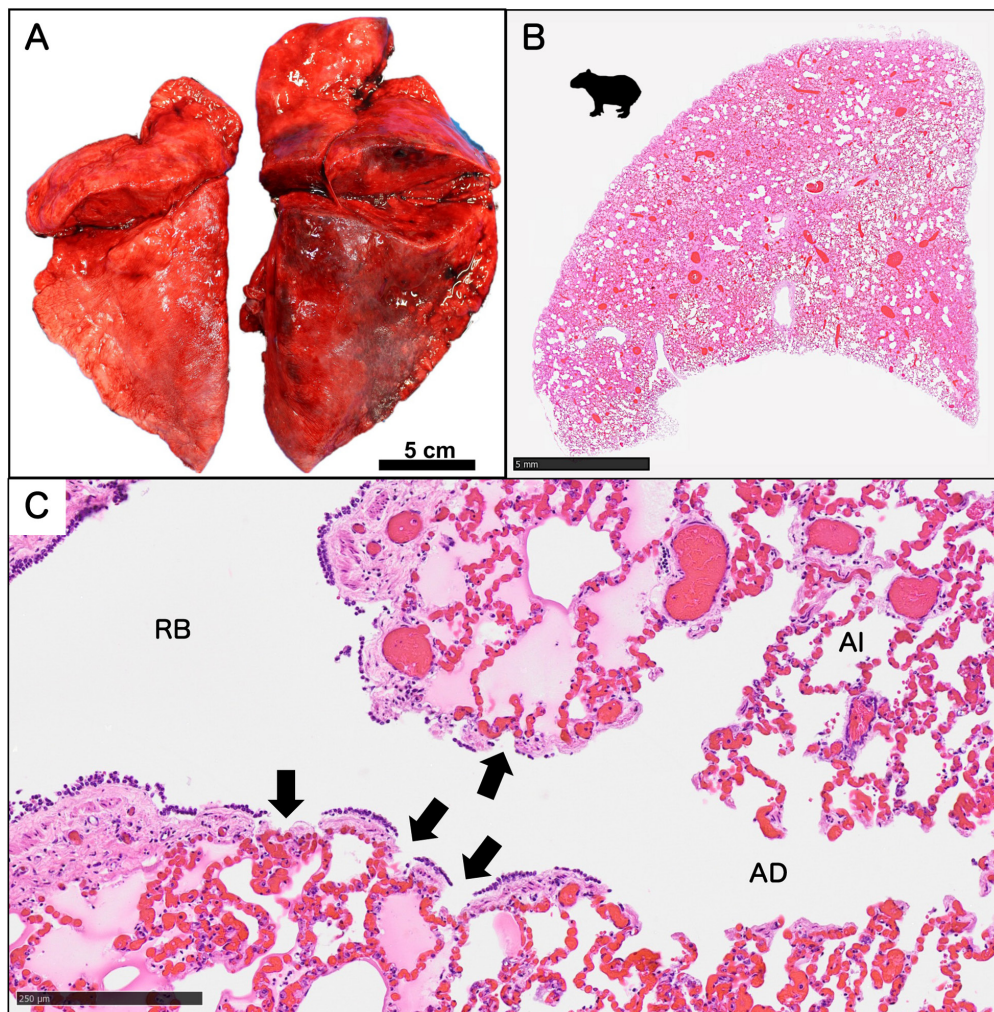


Fig. 4. Macroscopic and microscopic images of the capibara lung. A: Macroscopic image of a capibara lung. B: Microscopic image of the lung. C: High-magnification image of Fig. 4B showing the boundary between the bronchioles and alveoli. AD: alveolar duct; AI: alveoli; RB: respiratory bronchiole; arrow: alveoli associated with respiratory bronchioles.

the human lung is not observed on the surface of the lung (Fig. 5A). Consistent with this finding, the lungs do exhibit any lobular structures (Fig. 5B). However, the respiratory bronchioles are clearly visible (Fig. 5C, 5D; Table 1). Similarly, other members of the order Carnivora, such as Bengal tigers (*Panthera tigris tigris*), Japanese raccoon dogs (*Nyctereutes viverrinus viverrinus*), and Chinese wolves (*Canis lupus chanco*), lack septa but have prominent respiratory bronchioles (Table 1). Notably, cats (*Felis catus*) and ferrets (*Mustela putorius furo*) have respiratory bronchioles but lack interlobular septa, and ferrets in particular are considered to be better models for humans than rodents²³ (Table 2). Kock *et al.* found that inhalation exposure of rats, monkeys, and ferrets to ozone caused more severe acute damage to the lung epithelium in ferrets, which like humans and monkeys have respiratory bronchioles, than in rats³¹. As discussed above, some Carnivora have well-developed respiratory bronchioles and are useful models for human peripheral airways; however, as in mice and rats, they lack interlobular

septa and are consequently not appropriate models for assessing the effects of the septum on inhalation toxicity and disease.

Nonhuman Primates

In cynomolgus monkeys (*Macaca fascicularis*), a common primate used in research, the polygonal pattern present in human lungs is observed on the lung surface (Fig. 6A). Consistent with this finding, no lobular structures are observed in the lungs (Fig. 6B). However, respiratory bronchioles are clearly visible (Fig. 6C, 6D). The abundant presence of airway smooth muscle tissue in the bronchiolar structure, similar to that in humans, makes it easy to identify the alveolar structure of the respiratory bronchioles. The lung surfaces of the common marmoset (*Callithrix jacchus*) also shows neither a polygonal pattern (Fig. 7A) or microscopic interlobular septa (Fig. 7B). In contrast, respiratory bronchioles are readily visible (Fig. 7C). Similarly, in squirrel monkeys

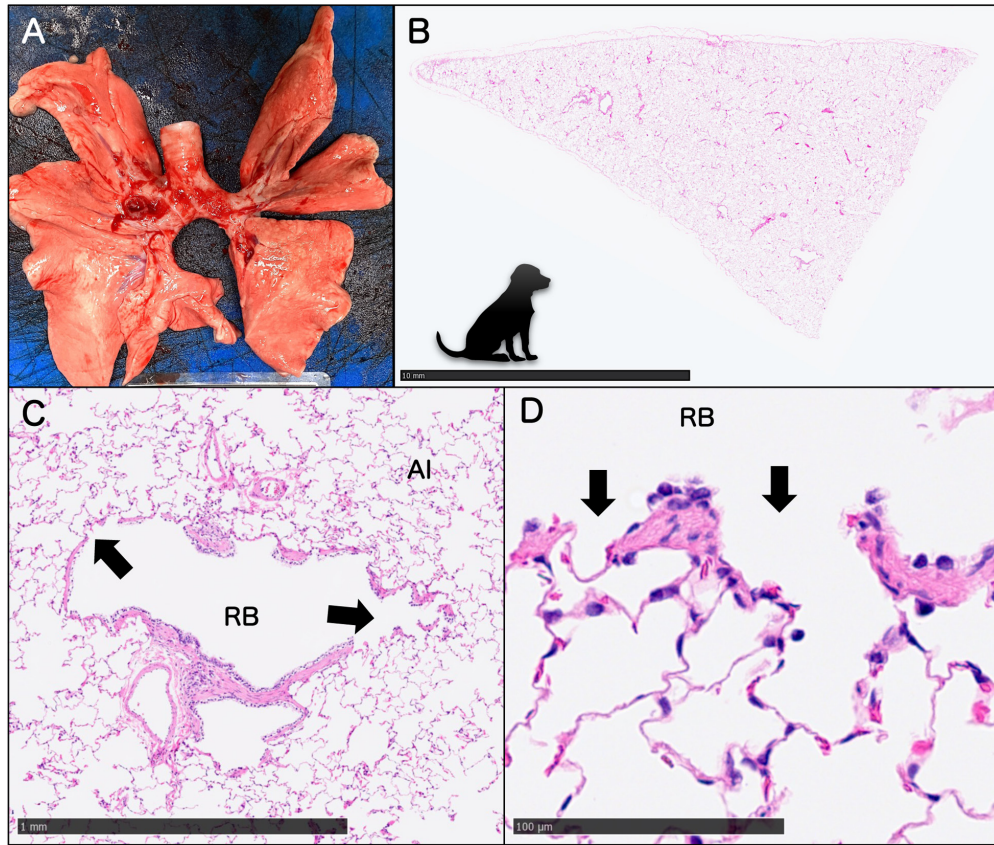


Fig. 5. Macroscopic and microscopic images of the dog lung. A: Macroscopic image of a beagle dog lung. B: Microscopic image of a beagle dog lung. C: High-magnification image of Fig. 5B showing the boundary between the bronchioles and alveoli. D: High-magnification image of Fig. 5C. AI: alveoli; RB: respiratory bronchioles; arrow: alveoli associated with respiratory bronchioles.

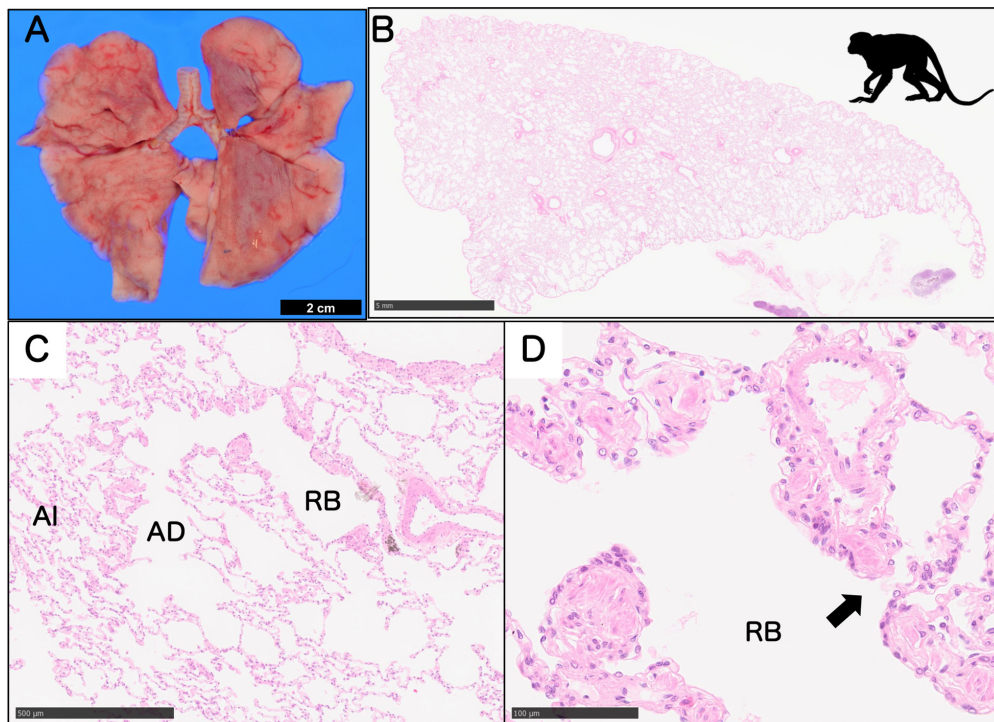


Fig. 6. Macroscopic and microscopic images of the cynomolgus monkey lung. A: Macroscopic image of a cynomolgus monkey lung. B: Microscopic image of a cynomolgus monkey lung. C: High-magnification image of Fig. 6B showing the boundary between the bronchioles and alveoli. D: High-magnification image of Fig. 6C. AD: alveolar duct; AI: alveoli; RB: respiratory bronchiole.

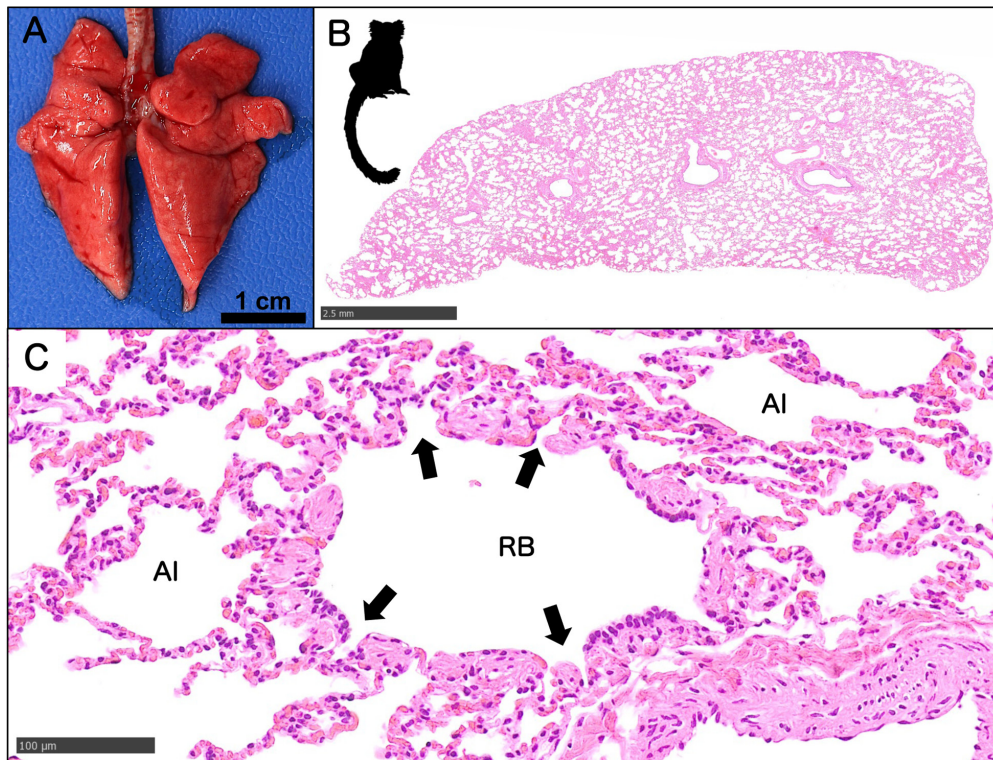


Fig. 7. Macroscopic and microscopic images of the common marmoset lung. A: Macroscopic image of a common marmoset lung. B: Microscopic image of a common marmoset lung. C: High-magnification image of Fig. 7B showing respiratory bronchioles. Al: alveoli; RB: respiratory bronchioles; arrow: alveoli associated with the respiratory bronchioles.

(*Saimiri sciureus*), we observed respiratory bronchioles, but not lobular structures (Table 1). Rhesus monkeys (*Macaca mulatta*)⁴³, the most commonly used nonhuman primate experimental animal in certain types of experiments, such as vaccine trials, have also been reported to have respiratory bronchioles but few interlobular septa^{23, 26} (Table 2). No clear anatomical differences were identified between the examined Old World monkeys (cynomolgus monkeys and rhesus monkeys) and New World monkeys (common marmosets and squirrel monkeys). Respiratory bronchioles are observed in both Old World and New World monkeys; however, no clear lobular structures are observed.

Cetartiodactyla

Both respiratory bronchioles and interlobular septa are present in pigs (*Sus scrofa domestica*) (Table 1). Figure 8A shows the appearance and lobular structure of the pig lung. The Microminipig⁴⁴, bred for research, displays a clear polygonal pattern on the lung surface (Fig. 8B, 8C) and well-defined interlobular septa (Fig. 8D). Histologically, the Microminipig lung is partitioned by thin connective tissue and vasculature (Fig. 8E–8I). Distal to the terminal bronchioles, respiratory bronchioles are observed where the bronchiolar epithelium and alveolar epithelium coexist supported by smooth muscle (Fig. 8I). Therefore, unlike rats and mice, pigs have a lung structure similar to that of humans

due to their prominent interlobular septa. The Mizo local pig, reared in the Mizoram highlands, has a thick visceral pleura and interlobular septa with elastic fibers, potentially enhancing lung elasticity, and well-developed respiratory bronchioles improving respiratory efficiency⁴⁵. This makes pigs sensitive models for studying diseases involving the interlobular septa.

Goat (*Capra Linnaeus*) lungs also exhibit both respiratory bronchioles and interlobular septa (Table 1). In goat lungs, a partial polygonal pattern is observed (Fig. 9A), and cross-sectional and histopathological examination reveals distinct interlobular septa in continuity with the pleura (Fig. 9C). However, while interlobular septa are present, the pattern of interlobular septa does not appear to be as well developed as in pigs (Fig. 9B). In contrast, respiratory bronchioles are more distinct in goats than in pigs (Fig. 9E).

In the lungs of cows (*Bos taurus*), both respiratory bronchioles and interlobular septa are prominent (Table 1). A polygonal pattern is observed macroscopically (Fig. 10A, 10B), and connective tissue and vasculature define interlobular septa histologically (Fig. 10C, 10D). Respiratory bronchioles with mixed bronchiolar epithelium and alveoli are also observed (Fig. 10E). The lungs of alpacas (*Vicugna pacos*) (Table 1) and camels (*Camelus Linnaeus*)^{27, 29}, two members of the family Camelidae, also contain both interlobular septa and respiratory bronchioles. Silicosis can develop in camels and, similarly to humans, is associated with diffuse

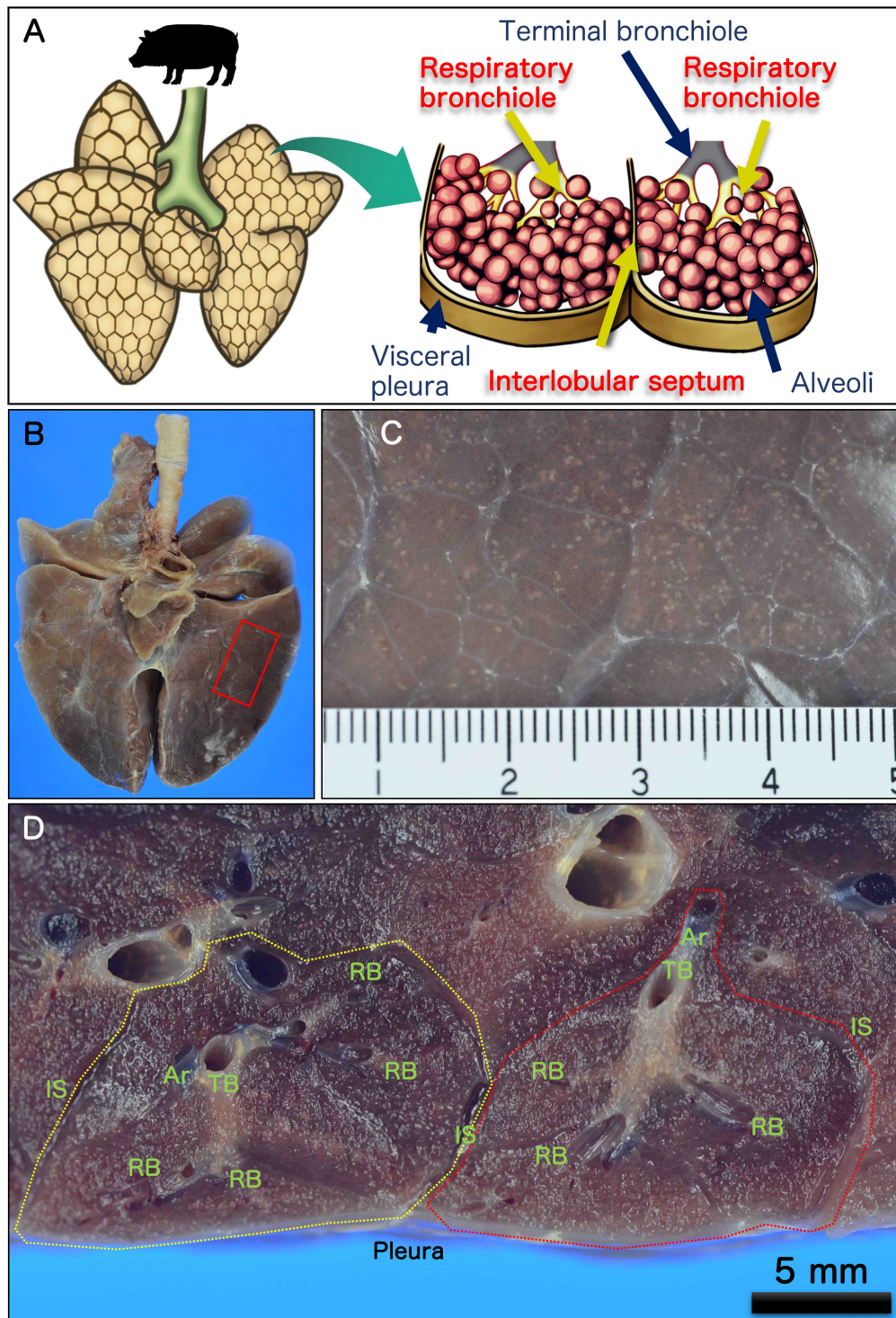


Fig. 8. Continued.

to nodular fibrosis due to dust accumulation, with thickened interlobular septa and interalveolar septa infiltrated by fibrous tissue and inflammatory cells²⁷. The lungs of reindeer (*Rangifer tarandus*) (Table 1), which belong to the family Cervidae, also possess both interlobular septa and respiratory bronchioles and may be suitable for the study of human occupational respiratory diseases. The lungs of sheep (*Ovis*

aries)²³ (Table 2), which belong to the goat subfamily, also have interlobular septa, but unlike goats, respiratory bronchioles are poorly developed.

In contrast, the pantropical spotted dolphin (*Stenella attenuata*), a marine Cetartiodactyla species, does not have respiratory bronchioles or lobular structures and also differs from humans in their bronchial and alveolar structures.

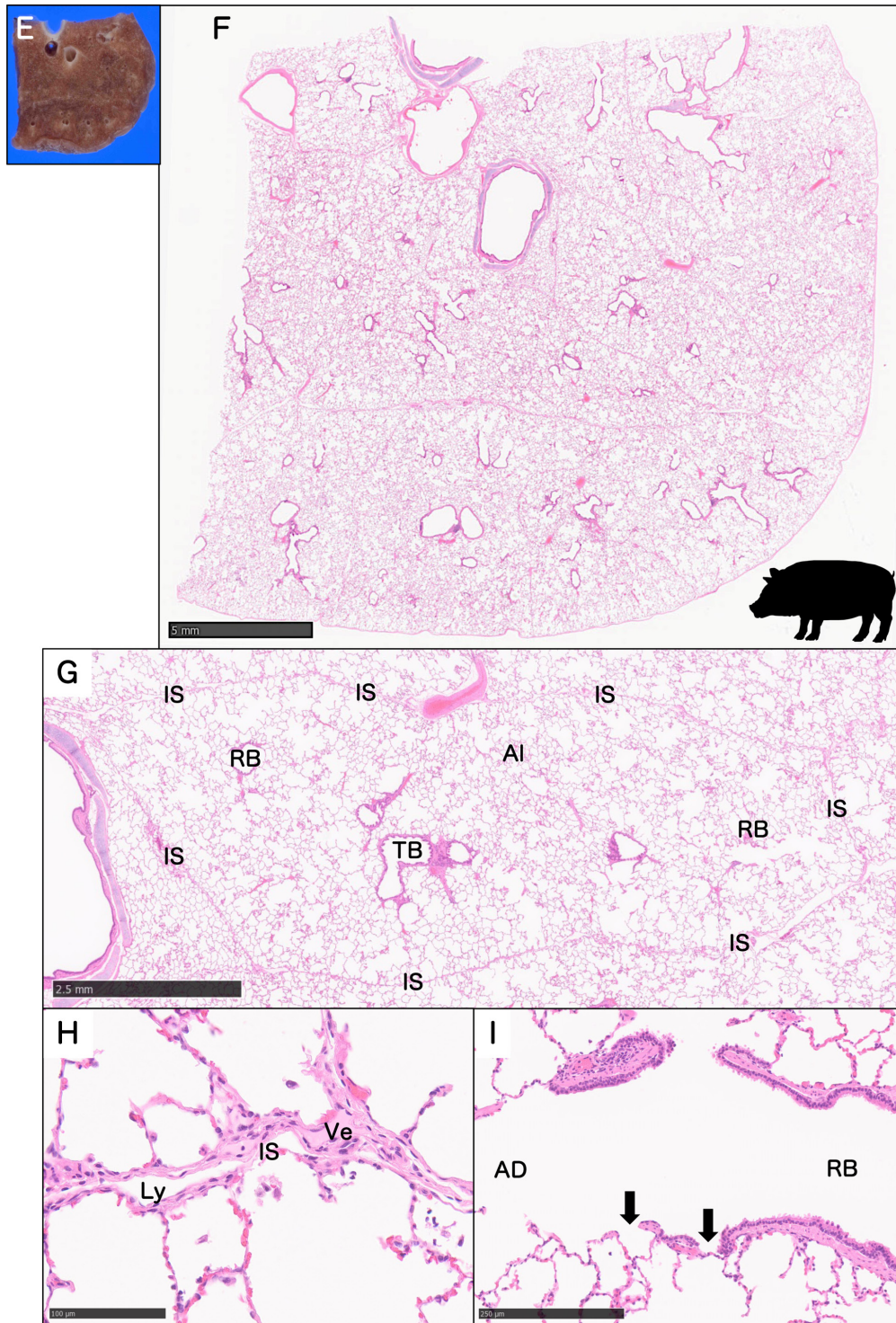


Fig. 8. Macroscopic and microscopic images of the Microminipig lung. A: Schematic of the lobular structure and peripheral airways of the pig lung. B: Overall view of the lung. C: High-magnification image of Fig. 8B showing a polygonal pattern on the surface of the lung. D: Lung tissue specimens. The red and yellow dotted lines indicate the lung lobules. E: The site of excision when preparing the pathological specimen. F: Microscopic image of a lung specimen showing prominent lobular structures and interlobular septa. G: Histological image showing distinct lobules surrounded by interlobular septa. H: Interlobular septa composed of interstitium containing lymphatic vessels and veins. I: Respiratory bronchioles. The bronchiolar epithelium and alveoli (arrows) are intermingled. Ar: artery; AD: alveolar duct; AI: alveoli; IS: interlobular septum; Ly: lymphatic vessel; RB: respiratory bronchiole; TB: terminal bronchiole; Ve: vein; arrow: alveoli associated with the respiratory bronchioles.

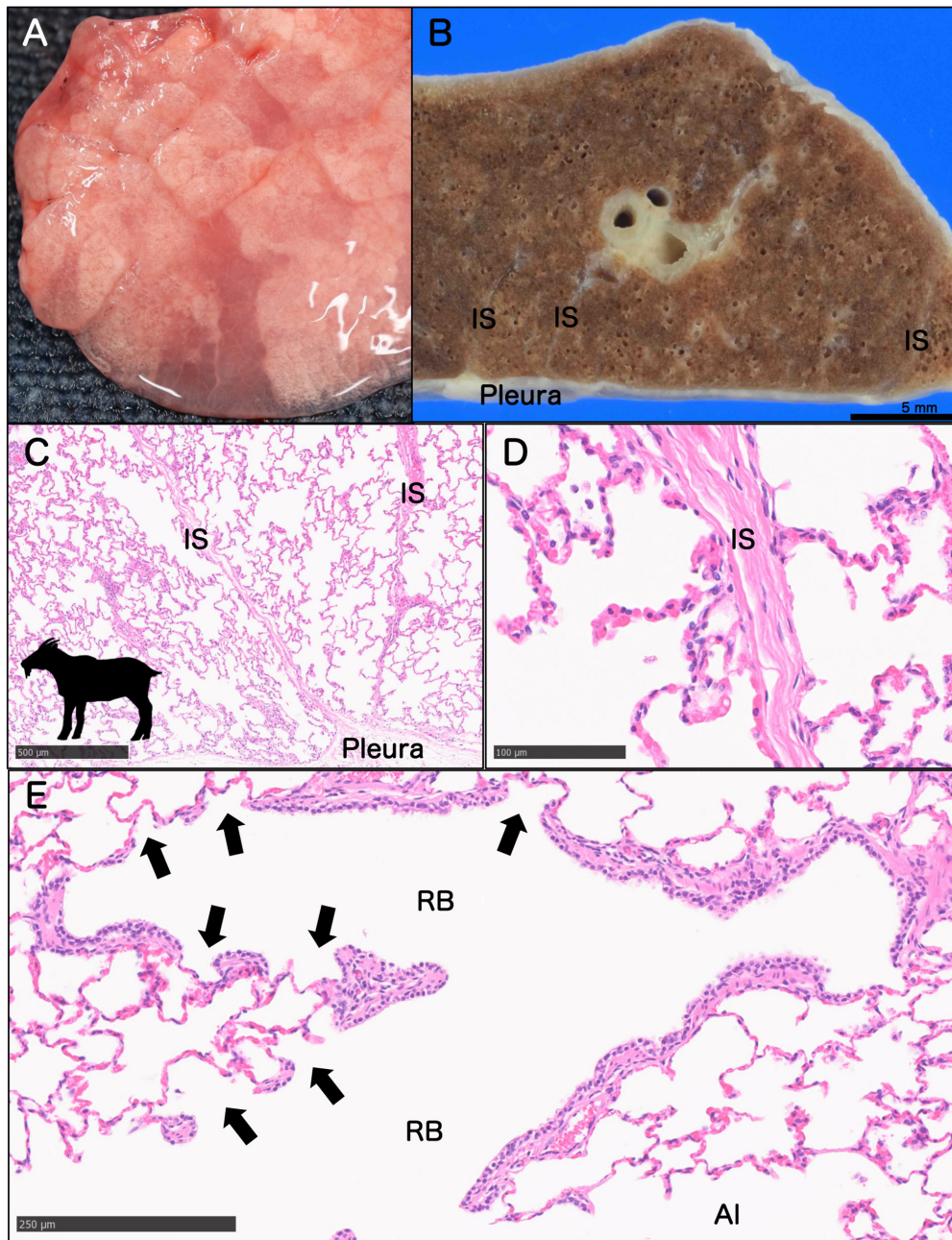


Fig. 9. Macroscopic and microscope images of the goat lung. A: Macroscopic high-magnification image of a goat lung showing a partial polygonal pattern on the lung surface. B: Lung tissue specimen. Interlobular septa continuous with the pleura are observed. C: Microscopic image of a goat lung specimen D: High-magnification image of Fig. 9C showing an interlobular septum continuous with the pleura. E: High magnification image of the lung of a goat showing the boundary between the bronchi and alveoli. Al: alveoli; IS: interlobular septum; RB: respiratory bronchiole; IS: interlobular septum; arrow: alveoli associated with respiratory bronchioles.

The bronchial and lung structure of the dolphin is shown in Fig. 11A. There is no clear lobular structure in dolphin lungs (Fig. 11B), whereas their terminal bronchioles and alveoli are distinct, with cartilage extending to the distal bronchioles (Fig. 11C). Numerous well-developed myoelastic sphincters (MES) formed circular expansions around the terminal bronchiole (Fig. 11C), creating constrictions (Fig. 11C, 11D). Unlike terrestrial species, dolphin alveoli have shallow depressions. This unique structure suggests

that the MES regulates airflow, protects the alveoli, and maintains gas exchange in this deep-sea marine species⁴⁶.

Other Species

In the order Perissodactyla, both donkeys (*Equus asinus*) and black rhinoceroses (*Diceros bicornis*) show a slight polygonal pattern on the lung surfaces (Table 1). Donkeys and black rhinoceroses have interlobular septa, but not

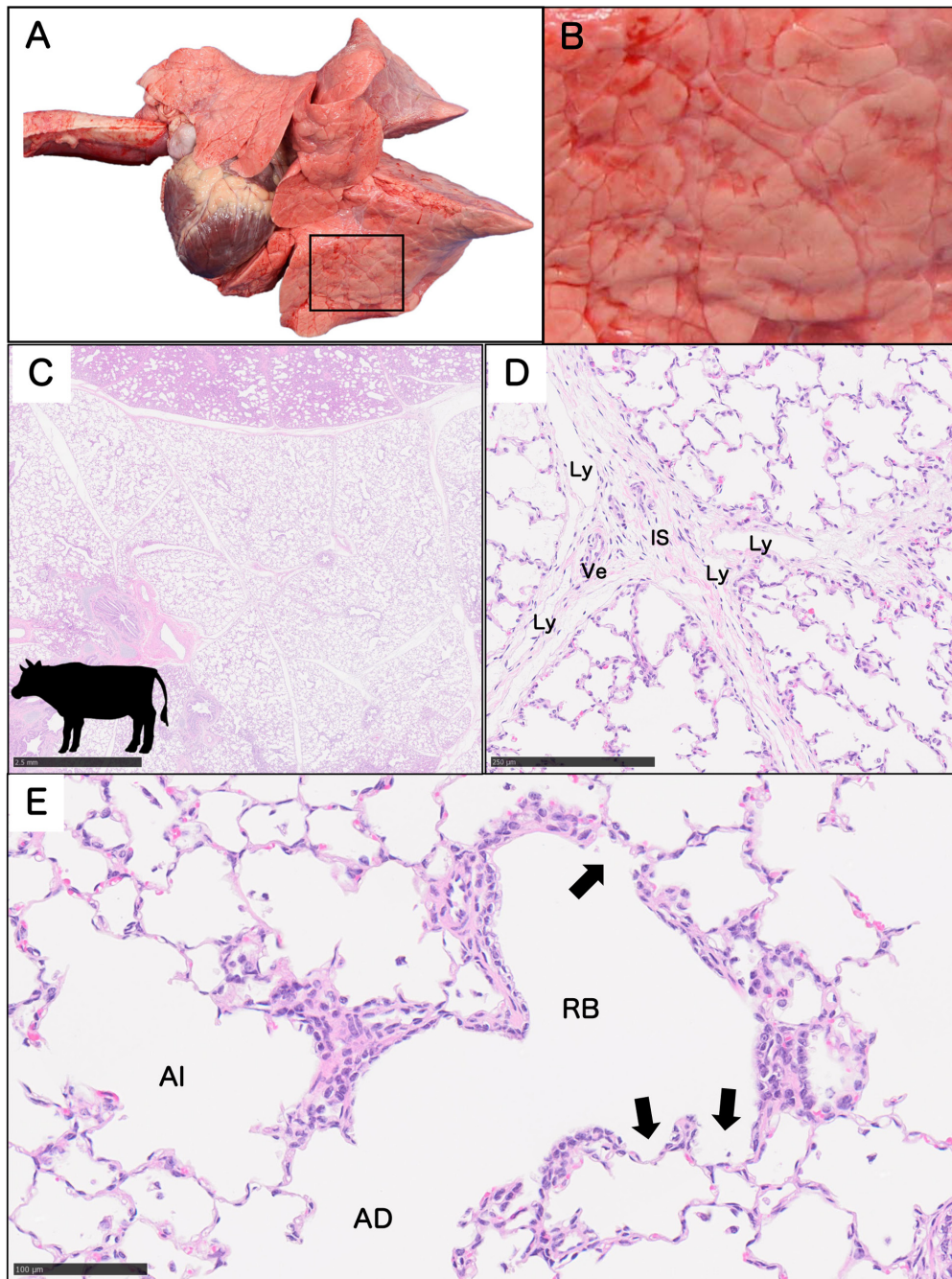


Fig. 10. Macroscopic and microscope images of the cow lung. A: Macroscopic image of a cow lung. B: Magnified view of the boxed area in panel A. C: Microscopic image of the lung showing prominent lobular structures and interlobular septa. D: High-magnification image of Fig. 10C showing the interlobular septum. E: High-magnification image of the lung of a cow showing the boundary between the bronchioles and alveoli. AD: alveolar duct; Al: alveoli; IS: interlobular septum; Ly: lymphatic vessel; RB: respiratory bronchiole; Ve: vein; arrow: alveoli associated with respiratory bronchioles.

as pronounced as in pigs, and respiratory bronchioles can not be resolved due to unclear bronchiole structures. Horses (*Equus caballus*) also have interlobular septa, but with incomplete septal separation of the lobules³⁰. In addition, the lungs of horses have been reported to be devoid of respiratory bronchioles (Table 2)³⁰.

In the order Marsupialia, koalas (*Phascolarctos cinereus*) do not have lobular structures, and the respiratory

bronchioles can not be resolved due to unclear bronchiole structures (Table 1).

Discussion and Conclusion

A cross-species investigation of respiratory bronchioles and lobular structures in over 30 mammalian species revealed species variation, with some species having these

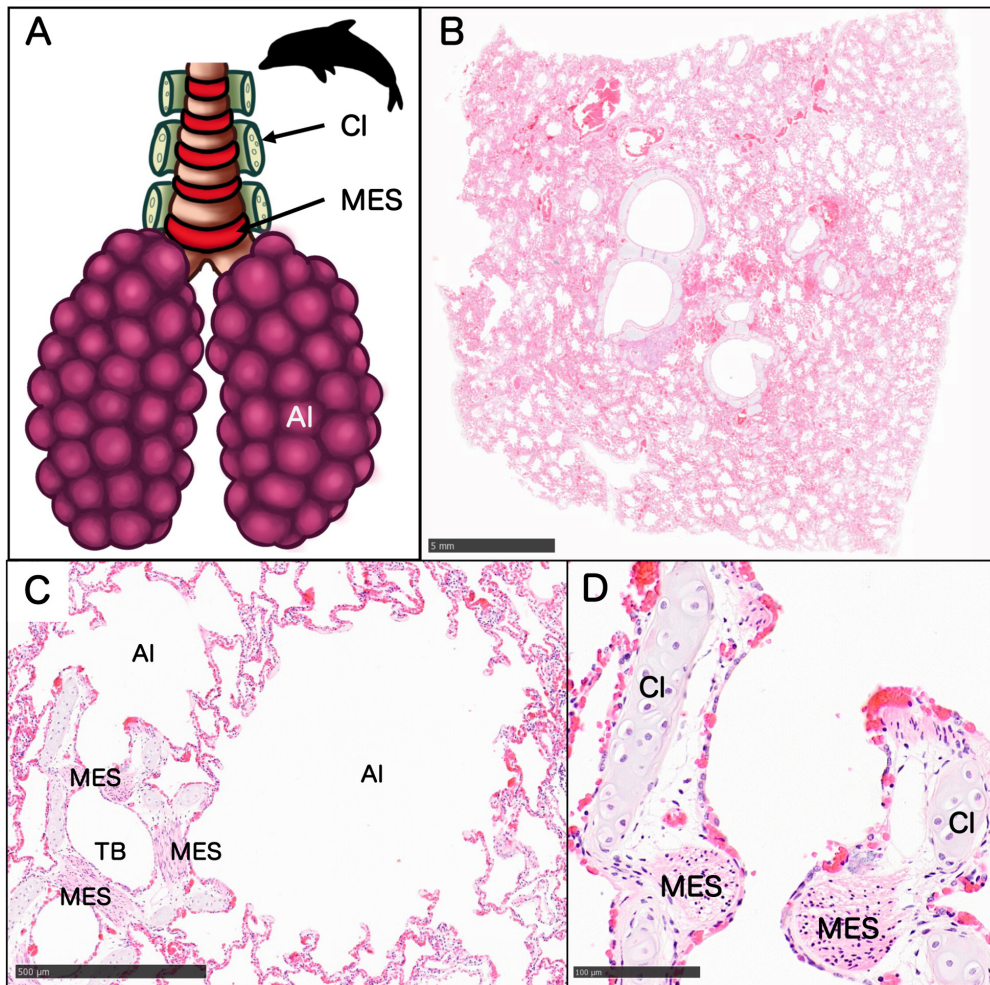


Fig. 11. Microscope images of the dolphin lung. A: Schematic of the terminal respiratory unit of the dolphin lung, with well-developed myoelastic sphincters and externally supported cartilage in the terminal bronchioles, a feature that makes it distinct from other mammals. B: Microscopic image of the lung. C: High-magnification image of Fig. 11B showing the boundary between the bronchiole and alveoli. D: High-magnification image of Fig. 11C. AI: alveoli; CI: cartilage; MES: myoelastic sphincters; TB: terminal bronchiole.

structures while others did not. None of the rodent species studied exhibit lobular structures. Notably, nonhuman primates show respiratory bronchioles but lack interlobular septa, confirming the absence of human-like lobular structures in these species. Similarly, carnivores show no discernible lobular structures. Therefore, terrestrial even-toed ungulates are reaffirmed as the only animals possessing both respiratory bronchioles and lobular structures, paralleling human respiratory anatomy.

Using pigs, particularly miniature pigs such as minipigs and Microminipigs, can bridge the gap between the results of rodent studies and human clinical studies, enhancing our understanding of respiratory diseases in humans. Minipigs are also used to study infectious diseases^{47, 48} and Chronic Obstructive Pulmonary Disease, a leading cause of human mortality^{49, 50}. Cystic fibrosis (CF), caused by mutations in the CF transmembrane conductance regulator gene (CFTR), also affects both humans and pigs^{51, 52}. In particular, CF studies of the lung using pigs have advantages over studies using mice because of their well-developed submu-

cosal glands^{53, 54}. Therefore, pigs have a lung structure suitable for evaluating human respiratory disease pathology and will be valuable for respiratory disease research, potentially accelerating early detection, treatment, and prevention of human respiratory diseases. Minipigs are commonly used in regulatory toxicity studies, with the Göttingen minipig being the preferred choice in Europe, and their use is accepted by regulatory authorities⁵⁵. In Europe, minipigs are increasingly replacing beagle dogs for safety pharmacology studies⁵⁵. Koch *et al.* at the Fraunhofer Institute in Germany have developed an inhalation model for Göttingen minipigs⁵⁶. This model includes a mask that ensures the precise and reproducible delivery of aerosols and gaseous substances to the airways. They also developed a head-only exposure system and demonstrated the particle-size dependence of lung deposition using a chemical tracer method⁵⁷.

Pigs have respiratory bronchioles and lobular structures, making them ideal models for studying occupational respiratory diseases such as pneumoconiosis. In addition to the ethical issues that must be considered when experi-

menting with nonhuman primates, miniature pigs are more suitable for inhalation studies of environmental hazards compared to nonhuman primates and beagle dogs. We are currently developing a technique to administer chemical suspensions directly into the lungs of pigs, similar to the intratracheal administration method used in rodents.

This review reconfirms that, aside from humans, only animals belonging to the terrestrial even-toed ungulate taxonomic branch have prominent respiratory bronchioles and lobular structures. Pigs have more pronounced lobular structures than humans, making them sensitive to changes, such as interlobular septa thickening. Goats have even more developed respiratory bronchioles than pigs, potentially making them more sensitive to lesions such as silicotic nodules and asbestos lung. The manageable size of miniature pigs and miniature goats makes them suitable for long-term experiments that induce chronic diseases, such as end-stage pulmonary fibrosis, lasting up to two years. We are planning a study in which Microminipigs will be administered asbestos and observed for two years to test the ability of this animal model to detect carcinogenicity.

Recent advancements such as single-cell RNA sequencing have identified novel cell subsets in the respiratory organs of both healthy and diseased humans, providing new insights into disease pathology^{58–62}. Studies have shown that AT0/RAS cells, which are particularly abundant in human respiratory bronchioles, are present in ferrets⁶³ and monkeys⁶⁴, but not in mice, highlighting significant species differences at the single-cell resolution level. We confirmed that these cell subsets are abundant in the lungs of Microminipigs (unpublished data).

Utilizing new research methods and selecting suitable experimental animals will advance our understanding of human respiratory diseases and lead to early detection, improved treatment, and preventive strategies.

Disclosure of Potential Conflicts of Interest: The authors have no competing interests to disclose.

Acknowledgments: We thank Misae Saito (National Institute for Occupational Safety and Health) for assistance with the preparation of the pathological specimens, Kinji Kobayashi (Shin Nippon Biomedical Laboratories, Ltd.) for providing the macroscopic figures and histopathological specimens of the beagle dog and cynomolgus monkey, and Aya Umeda for drawing the silhouette diagrams of the animals in the figures and the lung structures of the Microminipigs and dolphins. We received samples from the “Kumadai-Deba” naked mole-rat research sample supply system at Kumamoto University, with the support of Prof. Kyoko Miura. We also wish to thank Dr. David B. Alexander of the Nanotoxicology Project, Nagoya City University Graduate School of Medicine for his insightful comments and English language editing. This work was supported by JSPS KAKENHI (No. 23H03157 to SY) and a grant-in-aid from the Japan Organization of Occupational Health and Safety (Collaborative Research to YU).

References

1. West JB. How well designed is the human lung? *Am J Respir Crit Care Med.* **173**: 583–584. 2006. [Medline] [CrossRef]
2. West JB, Watson RR, and Fu Z. The human lung: did evolution get it wrong? *Eur Respir J.* **29**: 11–17. 2007. [Medline] [CrossRef]
3. Green FH, Vallyathan V, and Hahn FF. Comparative pathology of environmental lung disease: an overview. *Toxicol Pathol.* **35**: 136–147. 2007. [Medline] [CrossRef]
4. Snipes MB, McClellan RO, Mauderly JL, and Wolff RK. Retention patterns for inhaled particles in the lung: comparisons between laboratory animals and humans for chronic exposures. *Health Phys.* **57**(Suppl 1): 69–77, discussion 77–78. 1989. [Medline] [CrossRef]
5. Chen Q, Klein JS, Gamsu G, and Webb WR. High-resolution computed tomography of the mammalian lung. *Am J Vet Res.* **53**: 1218–1224. 1992. [Medline] [CrossRef]
6. Tata PR, and Rajagopal J. Plasticity in the lung: making and breaking cell identity. *Development.* **144**: 755–766. 2017. [Medline] [CrossRef]
7. Wansleeben C, Barkauskas CE, Rock JR, and Hogan BLM. Stem cells of the adult lung: their development and role in homeostasis, regeneration, and disease. *Wiley Interdiscip Rev Dev Biol.* **2**: 131–148. 2013. [Medline] [CrossRef]
8. Baron RM, Choi AJS, Owen CA, and Choi AMK. Genetically manipulated mouse models of lung disease: potential and pitfalls. *Am J Physiol Lung Cell Mol Physiol.* **302**: L485–L497. 2012. [Medline] [CrossRef]
9. Rock JR, Randell SH, and Hogan BLM. Airway basal stem cells: a perspective on their roles in epithelial homeostasis and remodeling. *Dis Model Mech.* **3**: 545–556. 2010. [Medline] [CrossRef]
10. DeLight N, and Sachs H. *Pneumoconiosis*. StatPearls Publishing, Treasure Island. 2024.
11. Pinkerton KE, Green FH, Saiki C, Vallyathan V, Plopper CG, Gopal V, Hung D, Bahne EB, Lin SS, Ménache MG, and Schenker MB. Distribution of particulate matter and tissue remodeling in the human lung. *Environ Health Perspect.* **108**: 1063–1069. 2000. [Medline] [CrossRef]
12. Mukhopadhyay S. *Non-Neoplastic Pulmonary Pathology: An Algorithmic Approach to Histologic Findings in the Lung*. Cambridge University Press, Cambridge. 2016.
13. Roggli VL, Gibbs AR, Attanoos R, Churg A, Popper H, Cagle P, Corrin B, Franks TJ, Galateau-Salle F, Galvin J, Hasleton PS, Henderson DW, and Honma K. Pathology of asbestosis—an update of the diagnostic criteria: report of the asbestosis committee of the college of American pathologists and pulmonary pathology society. *Arch Pathol Lab Med.* **134**: 462–480. 2010. [Medline] [CrossRef]
14. Wright JL, and Churg A. Morphology of small-airway lesions in patients with asbestos exposure. *Hum Pathol.* **15**: 68–74. 1984. [Medline] [CrossRef]
15. Katzenstein ALA. *Diagnostic Atlas of Non-Neoplastic Lung Disease: A Practical Guide for Surgical Pathologists*. Demos Medical, Syracuse. 2016.
16. Honma K, Abraham JL, Chiyotani K, De Vuyst P, Dumortier P, Gibbs AR, Green FHY, Hosoda Y, Iwai K, Williams WJ, Kohyama N, Ostiguy G, Roggli VL, Shida H, Taguchi O, and Vallyathan V. Proposed criteria for mixed-dust pneumoconiosis: definition, descriptions, and guidelines for pathologic diagnosis and clinical correlation. *Hum Pathol.*

- 35: 1515–1523. 2004. [\[Medline\]](#) [\[CrossRef\]](#)
17. Schraufnagel DE. Lung lymphatic anatomy and correlates. *Pathophysiology*. **17**: 337–343. 2010. [\[Medline\]](#) [\[CrossRef\]](#)
18. Sozio F, Rossi A, Weber E, Abraham DJ, Nicholson AG, Wells AU, Renzoni EA, and Sestini P. Morphometric analysis of intralobular, interlobular and pleural lymphatics in normal human lung. *J Anat*. **220**: 396–404. 2012. [\[Medline\]](#) [\[CrossRef\]](#)
19. Akira M. Uncommon pneumoconioses: CT and pathologic findings. *Radiology*. **197**: 403–409. 1995. [\[Medline\]](#) [\[CrossRef\]](#)
20. Kishimoto T, Okamoto K, Koda S, Ono M, Umeda Y, Yamano S, Takeda T, Rai K, Kato K, Nishimura Y, Kobashi Y, and Kawamura T. Respiratory disease in workers handling cross-linked water-soluble acrylic acid polymer. *PLoS One*. **18**: e0284837. 2023. [\[Medline\]](#) [\[CrossRef\]](#)
21. Takeda T, Yamano S, Goto Y, Hirai S, Furukawa Y, Kikuchi Y, Misumi K, Suzuki M, Takanobu K, Senoh H, Saito M, Kondo H, Daghliah G, Hong Y-K, Yoshimatsu Y, Hirashima M, Kobashi Y, Okamoto K, Kishimoto T, and Umeda Y. Dose-response relationship of pulmonary disorders by inhalation exposure to cross-linked water-soluble acrylic acid polymers in F344 rats. *Part Fibre Toxicol*. **19**: 27. 2022. [\[Medline\]](#) [\[CrossRef\]](#)
22. Yamano S, Takeda T, Goto Y, Hirai S, Furukawa Y, Kikuchi Y, Misumi K, Suzuki M, Takanobu K, Senoh H, Saito M, Kondo H, Kobashi Y, Okamoto K, Kishimoto T, and Umeda Y. Mechanisms of pulmonary disease in F344 rats after workplace-relevant inhalation exposure to cross-linked water-soluble acrylic acid polymers. *Respir Res*. **24**: 47. 2023. [\[Medline\]](#) [\[CrossRef\]](#)
23. Peake JL, and Pinkerton KE. Chapter 3—Gross and subgross anatomy of lungs, pleura, connective tissue septa, distal airways, and structural units. Academic Press, San Diego. 2015.
24. Miller WS. *The Lung*, 2nd edition. Charles C Thomas Publisher, Springfield. 1947.
25. Reid L. The secondary lobule in the adult human lung, with special reference to its appearance in bronchograms. *Thorax*. **13**: 110–115. 1958. [\[Medline\]](#) [\[CrossRef\]](#)
26. Tyler NK, Hyde DM, Hendrickx AG, and Plopper CG. Morphogenesis of the respiratory bronchiole in rhesus monkey lungs. *Am J Anat*. **182**: 215–223. 1988. [\[Medline\]](#) [\[CrossRef\]](#)
27. Goodarzi M, Azizi S, Koupaei MJ, and Moshkelani S. Pathologic findings of anthraco-silicosis in the lungs of one humped camels (*Camelus dromedarius*) and its role in the occurrence of pneumonia. *Kafkas Univ Vet Fak Derg*. 2013.
28. Abdel-Salam LR, Hussein FA, Gad MH, Khattal A-RAA, Elhawari WA, Amer AH, and Sherif DS. Light and scanning microscopic studies on the tracheobronchial epithelium of the one-humped camel (*camelus dromedarius*). *Med Res Chron*. **2**: 649–686. 2015.
29. He W, Zhang W, Cheng C, Li J, Wu X, Li M, Chen Z, and Wang W. The distributive and structural characteristics of bronchus-associated lymphoid tissue (BALT) in Bactrian camels (*Camelus bactrianus*). *PeerJ*. **7**: e6571. 2019. [\[Medline\]](#) [\[CrossRef\]](#)
30. Robinson N, and Furlow P. 1. Anatomy of the respiratory system. *Equine Respiratory Medicine and Surgery*. Elsevier, Philadelphia. 3–17. 2007.
31. Sterner-Kock A, Kock M, Braun R, and Hyde DM. Ozone-induced epithelial injury in the ferret is similar to nonhuman primates. *Am J Respir Crit Care Med*. **162**: 1152–1156. 2000. [\[Medline\]](#) [\[CrossRef\]](#)
32. Weibel ER. *Morphometry of the Human Lung*. Springer. Berlin, Heidelberg. 1963.
33. Davies A, and Moores C. Structure of the respiratory system, regard to function. *The Respiratory System* 11–28. 2010. [\[CrossRef\]](#)
34. Jeffery PK, and Li D. Airway mucosa: secretory cells, mucus and mucin genes. *Eur Respir J*. **10**: 1655–1662. 1997. [\[Medline\]](#) [\[CrossRef\]](#)
35. Miyata R, and van Eeden SF. The innate and adaptive immune response induced by alveolar macrophages exposed to ambient particulate matter. *Toxicol Appl Pharmacol*. **257**: 209–226. 2011. [\[Medline\]](#) [\[CrossRef\]](#)
36. Renne R, Brix A, Harkema J, Herbert R, Kittel B, Lewis D, March T, Nagano K, Pino M, Rittinghausen S, Rosenbruch M, Tellier P, and Wohrmann T. Proliferative and nonproliferative lesions of the rat and mouse respiratory tract. *Toxicol Pathol*. **37**(Suppl): 5S–73S. 2009. [\[Medline\]](#) [\[CrossRef\]](#)
37. Nagano K, Nishizawa T, Umeda Y, Kasai T, Noguchi T, Gotoh K, Ikawa N, Eitaki Y, Kawasumi Y, Yamauchi T, Arito H, and Fukushima S. Inhalation carcinogenicity and chronic toxicity of indium-tin oxide in rats and mice. *J Occup Health*. **53**: 175–187. 2011. [\[Medline\]](#) [\[CrossRef\]](#)
38. Umeda Y, Kasai T, Saito M, Kondo H, Toya T, Aiso S, Okuda H, Nishizawa T, and Fukushima S. Two-week toxicity of multi-walled carbon nanotubes by whole-body inhalation exposure in rats. *J Toxicol Pathol*. **26**: 131–140. 2013. [\[Medline\]](#) [\[CrossRef\]](#)
39. Kasai T, Umeda Y, Ohnishi M, Kondo H, Takeuchi T, Aiso S, Nishizawa T, Matsumoto M, and Fukushima S. Thirteen-week study of toxicity of fiber-like multi-walled carbon nanotubes with whole-body inhalation exposure in rats. *Nanotoxicology*. **9**: 413–422. 2015. [\[Medline\]](#) [\[CrossRef\]](#)
40. Kasai T, Umeda Y, Ohnishi M, Mine T, Kondo H, Takeuchi T, Matsumoto M, and Fukushima S. Lung carcinogenicity of inhaled multi-walled carbon nanotube in rats. *Part Fibre Toxicol*. **13**: 53. 2016. [\[Medline\]](#) [\[CrossRef\]](#)
41. Yamano S, Takeda T, Goto Y, Hirai S, Furukawa Y, Kikuchi Y, Kasai T, Misumi K, Suzuki M, Takanobu K, Senoh H, Saito M, Kondo H, and Umeda Y. No evidence for carcinogenicity of titanium dioxide nanoparticles in 26-week inhalation study in rasH2 mouse model. *Sci Rep*. **12**: 14969. 2022. [\[Medline\]](#) [\[CrossRef\]](#)
42. Yamano S, Goto Y, Takeda T, Hirai S, Furukawa Y, Kikuchi Y, Kasai T, Misumi K, Suzuki M, Takanobu K, Senoh H, Saito M, Kondo H, and Umeda Y. Pulmonary dust foci as rat pneumoconiosis lesion induced by titanium dioxide nanoparticles in 13-week inhalation study. *Part Fibre Toxicol*. **19**: 58. 2022. [\[Medline\]](#) [\[CrossRef\]](#)
43. Nogueira I, Català M, White AD, Sharpe SA, Bechini J, Prats C, Vilaplana C, and Cardona P-J. Surveillance of daughter micronodule formation is a key factor for vaccine evaluation using experimental infection models of tuberculosis in macaques. *Pathogens*. **12**: 236. 2023. [\[Medline\]](#) [\[CrossRef\]](#)
44. Kaneko N, Itoh K, Sugiyama A, and Izumi Y. Micromini-pig, a non-rodent experimental animal optimized for life science research: preface. *J Pharmacol Sci*. **115**: 112–114. 2011. [\[CrossRef\]](#)
45. Kalita A. Histomorphological study of the respiratory

- system of Mizo Local Pig (zo vawk). *Asian J Biomedical Pharm Sci* 4 2014. [\[CrossRef\]](#)
46. Piscitelli MA, Raverty SA, Lillie MA, and Shadwick RE. A review of cetacean lung morphology and mechanics. *J Morphol.* **274**: 1425–1440. 2013. [\[Medline\]](#) [\[CrossRef\]](#)
 47. Iwatsuki-Horimoto K, Nakajima N, Shibata M, Takahashi K, Sato Y, Kiso M, Yamayoshi S, Ito M, Enya S, Otake M, Kangawa A, da Silva Lopes TJ, Ito H, Hasegawa H, and Kawaoka Y. The microminipig as an animal model for influenza A virus infection. *J Virol.* **91**: e01716–e16. 2017. [\[Medline\]](#) [\[CrossRef\]](#)
 48. Ramos L, Obregon-Henao A, Henao-Tamayo M, Bowen R, Lunney JK, and Gonzalez-Juarrero M. The minipig as an animal model to study mycobacterium tuberculosis infection and natural transmission. *Tuberculosis (Edinb).* **106**: 91–98. 2017. [\[Medline\]](#) [\[CrossRef\]](#)
 49. Skydsgaard M, Dincer Z, Haschek WM, Helke K, Jacob B, Jacobsen B, Jeppesen G, Kato A, Kawaguchi H, McKeag S, Nelson K, Rittinghausen S, Schaudien D, Vemireddi V, and Wojcinski ZW. International Harmonization of Nomenclature and Diagnostic Criteria (INHAND): nonproliferative and proliferative lesions of the minipig. *Toxicol Pathol.* **49**: 110–228. 2021. [\[Medline\]](#) [\[CrossRef\]](#)
 50. Chen P, Hou J, Ding D, Hua X, Yang Z, and Cui L. Lipopolysaccharide-induced inflammation of bronchi and emphysematous changes of pulmonary parenchyma in miniature pigs (*Sus scrofa domestica*). *Lab Anim (NY).* **42**: 86–91. 2013. [\[Medline\]](#) [\[CrossRef\]](#)
 51. Stoltz DA, Meyerholz DK, Pezzulo AA, Ramachandran S, Rogan MP, Davis GJ, Hanfland RA, Wohlford-Lenane C, Dohrn CL, Bartlett JA, Nelson GA 4th, Chang EH, Taft PJ, Ludwig PS, Estin M, Hornick EE, Launspach JL, Samuel M, Rokhlina T, Karp PH, Ostedgaard LS, Uc A, Starner TD, Horswill AR, Brogden KA, Prather RS, Richter SS, Shilyansky J, McCray PB Jr, Zabner J, and Welsh MJ. Cystic fibrosis pigs develop lung disease and exhibit defective bacterial eradication at birth. *Sci Transl Med.* **2**: 29ra31–29ra31. 2010. [\[Medline\]](#) [\[CrossRef\]](#)
 52. Rogers CS, Hao Y, Rokhlina T, Samuel M, Stoltz DA, Li Y, Petroff E, Vermeer DW, Kabel AC, Yan Z, Spate L, Wax D, Murphy CN, Rieke A, Whitworth K, Linville ML, Korte SW, Engelhardt JF, Welsh MJ, and Prather RS. Production of CFTR-null and CFTR-DeltaF508 heterozygous pigs by adeno-associated virus-mediated gene targeting and somatic cell nuclear transfer. *J Clin Invest.* **118**: 1571–1577. 2008. [\[Medline\]](#) [\[CrossRef\]](#)
 53. Semaniakou A, Croll RP, and Chappe V. Animal models in the pathophysiology of cystic fibrosis. *Front Pharmacol.* **9**: 1475. 2019. [\[Medline\]](#) [\[CrossRef\]](#)
 54. Yan Z, Stewart ZA, Sinn PL, Olsen JC, Hu J, McCray PB Jr, and Engelhardt JF. Ferret and pig models of cystic fibrosis: prospects and promise for gene therapy. *Hum Gene Ther Clin Dev.* **26**: 38–49. 2015. [\[Medline\]](#) [\[CrossRef\]](#)
 55. Bode G, Clausen P, Gervais F, Loegsted J, Luft J, Nogues V, Sims J. Steering Group of the RETHINK Project. The utility of the minipig as an animal model in regulatory toxicology. *J Pharmacol Toxicol Methods.* **62**: 196–220. 2010. [\[Medline\]](#) [\[CrossRef\]](#)
 56. Koch W, Windt H, Walles M, Borlak J, and Clausen P. Inhalation studies with the Göttingen minipig. *Inhal Toxicol.* **13**: 249–259. 2001. [\[Medline\]](#) [\[CrossRef\]](#)
 57. Windt H, Kock H, Runge F, Hübel U, and Koch W. Particle deposition in the lung of the Göttingen minipig. *Inhal Toxicol.* **22**: 828–834. 2010. [\[Medline\]](#) [\[CrossRef\]](#)
 58. Hewitt RJ, and Lloyd CM. Regulation of immune responses by the airway epithelial cell landscape. *Nat Rev Immunol.* **21**: 347–362. 2021. [\[Medline\]](#) [\[CrossRef\]](#)
 59. Luecken MD, Zaragosi L-E, Madisoos E, Sikkema L, Firsova AB, De Domenico E, Kümmerle L, Saglam A, Berg M, Gay ACA, Schniering J, Mayr CH, Abalo XM, Larsson L, Sountoulidis A, Teichmann SA, van Eunen K, Koppelman GH, Saeb-Parsy K, Leroy S, Powell P, Sarkans U, Timens W, Lundeberg J, van den Berge M, Nilsson M, Horváth P, Denning J, Papatheodorou I, Schultze JL, Schiller HB, Barbry P, Petoukhov I, Misharin AV, Adcock IM, von Papen M, Theis FJ, Samakovlis C, Meyer KB, and Nawijn MC. The discovAIR project: a roadmap towards the Human Lung Cell Atlas. *Eur Respir J.* **60**: 2102057. 2022. [\[Medline\]](#) [\[CrossRef\]](#)
 60. Sikkema L, Ramírez-Suástegui C, Strobl DC, Gillett TE, Zappia L, Madisoos E, Markov NS, Zaragosi L-E, Ji Y, Ansari M, Arguel M-J, Apperloo L, Banchero M, Bécavin C, Berg M, Chichelnitskiy E, Chung MI, Collin A, Gay ACA, Gote-Schniering J, Hooshar Kashani B, Inecik K, Jain M, Kapellos TS, Kole TM, Leroy S, Mayr CH, Oliver AJ, von Papen M, Peter L, Taylor CJ, Walzthoeni T, Xu C, Bui LT, De Donno C, Dony L, Faiz A, Guo M, Gutierrez AJ, Heumos L, Huang N, Ibarra IL, Jackson ND, Kadur Lakshminarasimha Murthy P, Lotfollahi M, Tabib T, Talavera-López C, Travaglini KJ, Wilbrey-Clark A, Worlock KB, Yoshida M, van den Berge M, Bossé Y, Desai TJ, Eickelberg O, Kaminski N, Krasnow MA, Lafyatis R, Nikolic MZ, Powell JE, Rajagopal J, Rojas M, Rozenblatt-Rosen O, Seibold MA, Sheppard D, Shepherd DP, Sin DD, Timens W, Tsankov AM, Whitsett J, Xu Y, Banovich NE, Barbry P, Duong TE, Falk CS, Meyer KB, Kropski JA, Pe'er D, Schiller HB, Tata PR, Schultze JL, Teichmann SA, Misharin AV, Nawijn MC, Luecken MD, Theis FJ. Lung Biological Network Consortium. An integrated cell atlas of the lung in health and disease. *Nat Med.* **29**: 1563–1577. 2023. [\[Medline\]](#) [\[CrossRef\]](#)
 61. Tsukui T, Wolters PJ, and Sheppard D. Alveolar fibroblast lineage orchestrates lung inflammation and fibrosis. *Nature.* **631**: 627–634. 2024. [\[Medline\]](#) [\[CrossRef\]](#)
 62. Lin B, Shah VS, Chernoff C, Sun J, Shipkovenska GG, Vinarsky V, Waghray A, Xu J, Leduc AD, Hintschich CA, Surve MV, Xu Y, Capen DE, Villoria J, Dou Z, Hariri LP, and Rajagopal J. Airway hillocks are injury-resistant reservoirs of unique plastic stem cells. *Nature.* **629**: 869–877. 2024. [\[Medline\]](#) [\[CrossRef\]](#)
 63. Basil MC, Cardenas-Diaz FL, Kathiriya JJ, Morley MP, Carl J, Brumwell AN, Katzen J, Slovik KJ, Babu A, Zhou S, Kremp MM, McCauley KB, Li S, Planer JD, Hussain SS, Liu X, Windmueller R, Ying Y, Stewart KM, Oyster M, Christie JD, Diamond JM, Engelhardt JF, Cantu E, Rowe SM, Kotton DN, Chapman HA, and Morrissey EE. Human distal airways contain a multipotent secretory cell that can regenerate alveoli. *Nature.* **604**: 120–126. 2022. [\[Medline\]](#) [\[CrossRef\]](#)
 64. Kadur Lakshminarasimha Murthy P, Sontake V, Tata A, Kobayashi Y, Macadlo L, Okuda K, Conchola AS, Nakano S, Gregory S, Miller LA, Spence JR, Engelhardt JF, Boucher RC, Rock JR, Randell SH, and Tata PR. Human distal lung maps and lineage hierarchies reveal a bipotent progenitor. *Nature.* **604**: 111–119. 2022. [\[Medline\]](#) [\[CrossRef\]](#)